INL/JOU-18-51305-Revision-0

Lanthanide Migration and Immobilization in Metallic Fuels

Yi Xie, Jinsuo Zhang, Xiang Li, Jeremy Isler, Michael T Benson, Robert D Mariani, Cetin Unal

November 2018

The INL is a U.S. Department of Energy National Laboratory
operated by Battelle Energy Alliance

INL/JOU-18-51305-Revision-0

Lanthanide Migration and Immobilization in Metallic Fuels

Yi Xie, Jinsuo Zhang, Xiang Li, Jeremy Isler, Michael T Benson, Robert D Mariani, Cetin Unal

November 2018

Idaho National Laboratory
Idaho Falls, Idaho 83415

http://www.inl.gov

Prepared for the
U.S. Department of Energy
Office of Nuclear Energy, Office of Nuclear Energy
Under DOE Idaho Operations Office
Contract DE-AC07-05ID14517, DE-AC07-05ID14517

Lanthanide Migration and Immobilization in Metallic Fuels

Yi Xie[a], Jinsuo Zhang[a]*, Xiang Li[b], Jeremy P. Isler[b], Michael T. Benson[c], Robert D. Mariani[c], Cetin Unal[d]

a. Nuclear Engineering Program, Mechanical Engineering Department, Virginia Tech, Blacksburg, VA 24060, US

b. Nuclear Engineering Program, Ohio State University, Columbus, OH 43210, US

c. Idaho National Laboratory, P.O. Box 1625, MS 6188, Idaho Falls, ID 83415, US

d. Los Alamos National Laboratory, P.O. Box 1663, Los Alamos, NM 87545, US

**Corresponding author, Email: zjinsuo5@vt.edu, Phone: (540) 231-1198, Postal address: 635 Prices Fork Rd, Blacksburg, VA 24060, US*

Abstract

It is recognized that the lanthanide fission products can enhance the fuel-cladding chemical interaction (FCCI), which is a key concern of using metallic fuels such as U-Zr in a sodium-cooled fast reactor. The present work conducts a critical review on the analysis of lanthanide functions in FCCIs. Available in-pile and out-of-pile data are first collected and analyzed, then the theories for lanthanide migration and redistribution in the fuel in operation are analyzed. For mitigating FCCIs, one of the effective method is applying fuel additives for immobilizing lanthanides. The review investigates four candidates of fuel additives (Pd, Sn, Sb and In), and it is concluded that Sb can be the best candidate among the four elements based on current available thermodynamic data and microstructure characterizations. Considering that FCCIs lead to formation of metallic alloys/compounds between lanthanides and steel cladding constituents (Fe, Cr, and Ni), the review also analyzes the thermodynamic data such as enthalpy of formation of the alloys and/or metallic compounds and identify the solidus temperature of each alloy.

Key words: FCCI; Metallic fuel; Lanthanide migration; Lanthanide immobilization

1. Introduction

The selection by the Generation IV International Forum of sodium-cooled fast reactor concept has brought metallic fuels, such as U-Zr fuel, under renewed focus [1]. Metallic U-Zr fuels have shown advantageous capabilities, including a high thermal conductivity, high fissile atom density, easy fabrication, and pyroprocessing capability. Along with these properties, metallic fuels have shown good performance on both steady state and transient operating conditions of sodium-cooled fast reactors by experiments performed with the experimental breeder reactor II (EBR-II) [2]. The metallic fuel pin is comprised of rod-shaped fuel alloy made of U-Fs[1], U-Zr or U-Pu-Zr, the fuel-to-clad gap filled with liquid sodium (Na), and steel cladding HT9[2] [2]. The fuel pin is designed to allow for fuel swelling within the fuel-to-clad gap, and fission gas accumulating in the top plenum during reactor operation.

One of the earliest developments on metallic fuels was alloying. Some of the earliest alloying additions included molybdenum (Mo) and fissium (Fs). Later, Zr became the alloying element for metallic fuel in the use of EBR-II and fast flux test facility (FFTF) [3]. Alloying with Zr presents the ability to raise the solidus temperature of fuel, increase the compatibility between cladding and fuel, and increase the dimensional stability of metallic fuel under irradiation. It has been identified that the best composition of Zr is 10 wt. % in the fuel [5]. Although fuel alloying can increase the dimensional stability of metallic fuels under irradiation, design refinement of fuel element is still desired to reduce the effects of fuel swelling and chemical interactions between fuel and cladding.

At the beginning of metallic fuel development, the fuel-to-clad gap was relatively small, so large stresses were generated when fuel swells even at very low burnups (~3 at. %) [4]. Failures

[1] Fs (fissium) is composed of Ru, Mo, Pd, Te, Rh, Nb and Zr.

[2] Alloy HT9 is composite of 12 Cr, 1 Mo (wt. %), other minor elements such as Ni and C, and Fe as balance.

from the fuel imposing stresses on the cladding is known as fuel-cladding mechanical interaction (FCMI). To overcome FCMI, the designed thickness of fuel-to-clad gap was increased. The smear density was decreased to 75 % to allow the fuel with more initial unconstrained swelling to prevent failures caused by FCMI [5]. With 75 % smear density, an adequate amount of swelling occurs with the porosity developing in the fuel to form interconnected pathways from the fuel to the gap. The interconnected pathways allow fission gas to release from the fuel and to accumulate in the plenum at the upper portion of fuel pin. The release of fission gas eliminates one of the largest contributors to swelling. The design of smaller smear density has alleviated FCMI and achieved higher burnups.

As allowing the fuel to swell, the transformations associated with higher burnups have become a significant focus. Figure 1a is an optical micrograph, showing these transformations of the EBR-II irradiated U-23Zr wt. % fuel element T225 with D9[3] cladding at a burnup of 10 at. % [6]. Figure 1b is a schematic image of an irradiated fuel with several microstructure transformations of interest illustrated, including swelling, porosity, and constituent redistribution. Porosity developing in the swelling fuel is just one of many microstructure evolutions at high burnups. The other microstructure evolution was constituent redistribution in U-Zr fuels during reactor operation. Constituent redistribution results in a relatively higher Zr concentration at the fuel radial center and peripheral regions, while a higher U concentration at the intermediate regions. Previous work has shown that radial temperature gradients generated in rod-type fuel elements appear to be sufficiently large to cause redistribution of fuel constituents [7]. The constituent redistribution in U-Zr fuels has some advantages: the increased Zr concentration at the center may improve the solidus temperature of the hottest part of fuel,

[3] Alloy D9 is composite of 15.5 Ni, 13.5 Cr, 2 Mn, 2 Mo (wt. %), other minor elements such as Si and C, and Fe as balance.

and the increased Zr concentration at the periphery may increase the chemical compatibility between fuel and cladding. However, the disadvantage of redistribution is also critical as which would result in porosity and void formation in the fuel.

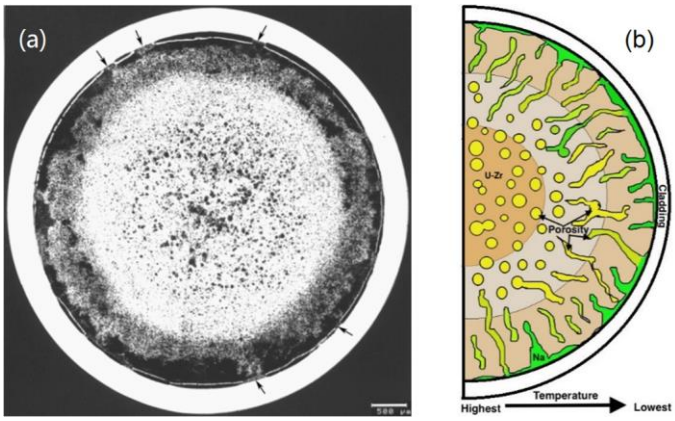

Figure 1 Transformations of post-irradiation U-Zr fuel. (a) Optical micrograph of fuel cross section [6], and (b) schematic diagram of half cross section with fuel transformations [8].

The swelling at the inner hottest region of fuel is dominated by the formation and growth of fission gas bubbles; while at the outer colder region is dominated by the tearing and cavity formation at grain boundaries. In addition to the various swelling mechanisms, the amount of swelling differs as well. The differences of swelling occurring at different regions result in the overall fuel swelling anisotropic and cracks growing at the fuel periphery [9]. Caused by the cracks, cavities and fission gas bubbles, the U-Zr fuel may develop a pathway of porosity, which connects from the fuel interior to the fuel-to-clad gap. This interconnected porosity is one of key features in the release of fission gas and the elimination of FCMI. Furthermore, the interconnected porosity is the migration path of lanthanide (Ln) fission products, the chemistry of which plays an important role in fuel-cladding chemical interaction (FCCI) [10].

Metallic U-Zr fuels have been used in EBR-II and qualified up to a burnup of 10 at. %, however, such a burnup is still far below the desired burnup of 20 at. % for the advanced sodium-cooled fast reactor [11]. A major reason for the limitation of higher burnup is FCCI, which occurs at

the fuel/cladding interface during irradiation [12]. FCCIs include fuel-cladding interactions (e.g. U-Fe) and lanthanide-cladding interactions (e.g. Ce-Fe). These chemical interactions may lead to cladding wastage with the formation of low temperature eutectics and brittle intermetallics. Low temperature eutectics composite of fuel constituents (U, Pu and Zr) and cladding constituents (Fe and Cr) have been found [13,14]. Liquefaction and liquid-phase penetration to cladding have been found during irradiation, the liquefied region is coincided with the Fe diffusion depth, the liquefaction threshold temperature is dependent on fuel composition and burnup [15,16]. However, the greatest concern of FCCI is lanthanide-cladding interactions, as lanthanides migrate fast in a fuel and diffuse rapidly into cladding. The present review is focused on the behavior of lanthanides in U-Zr metallic fuels during irradiation, which is different with the previous FCCI reviews (e.g. [14]).

2. Lanthanides at fuel/clad interface

Section 2.1 presents the post-irradiation behavior of lanthanide at the fuel/clad interface. Irradiation may enhance diffusion kinetics, thereby these results are different with the out-of-pile results; however, in-pile tests are limit, it's necessary to understand the chemical interactions of lanthanide and cladding through diffusion couple tests, which is discussed in Section 2.2.

2.1 In-pile data analysis

Both fission yield and fission product decay during the post-irradiation period have an influence on the abundance of lanthanide fission products [17]. As indicated by a sample composition of an irradiated U-10Zr fuel pin at around 8 at. % burnup [18], the vast majority compositions of lanthanide fission products are Nd, Ce, Pr and La. Fission products that are relatively insoluble in the U-Zr fuel matrix have been found as precipitates in the pores of fuel, such as Ce precipitates [12][19][20]. The solubility of Ce in metallic fuel at the typical fuel irradiation temperature (923-973 K) is very low, therefore most of Ce that produced during burning is

precipitated. Lanthanides have been experimentally found precipitated in the pores of fuel [20], and they are the major fission products at the outer region of metallic fuels during irradiation [21]. The temperature gradient in metallic fuel appears to play an important role in the lanthanide migration to the periphery [6] because the isothermal diffusion couple tests of lanthanide-contained fuel did not show lanthanide migration to the fuel surface [22]. Lanthanide precipitates at the fuel periphery have been found even at low burnups, indicating the migration is rapid [23].

Post irradiation examination (PIE) data of metallic fuels (U-Zr and U-Pu-Zr) irradiated in EBR-II reactor have been well summarized in the report [6]. The report found that some lanthanides (e.g. Nd, Ce, Pr, La, Sm and Pd) that were originally in the fuel finally were found in the cladding, indicating the occurrence of interdiffusion between lanthanides and cladding when fuel swells. Reports [6,11] also suggested Nd, Ce, Pr and La as four major lanthanides diffusing into cladding.

The formation of liquid-phase is one of the major type of cladding degradation during FCCI. The liquid phase region coincides with the depth of Fe migration from the cladding as shown from microprobe analysis, the addition of Fe diffusion can form more liquid phase during the test at elevated temperatures [16]. Tsai, et al. reported that the interdiffusion layers on the fuel and cladding inner surface may liquefy, resulting in liquid-phase penetration into the cladding at a high temperature [15]. Results from the fuel behavior test apparatus (FBTA) on EBR-II fuel pins showed that noticeable liquid phase penetration occurred at temperatures higher than 998 K and two types of interactions, grain boundary penetration and matrix dissolution [15]. Cohen, et al. also reported the threshold temperatures for fuel-cladding interaction melting in a 1-h test on a U-19Pu-l0Zr/HT9 element is 1013-1043 K for a 5.6 at. % burnup element, and 923-948 K for an 11 at. % burnup element [16]. The temperature threshold is impacted by the constituent near the fuel/clad interface. More Fe concentration in the fuel caused by the increased burnup

may contribute to the lower threshold temperature, depending on the equilibrium phase diagram of the new metallic system.

The cladding penetration rate in the steel cladding is significantly impacted by the existence of lanthanide fission products in the fuel/clad gap [15]. This is consistent with the observation from DP-1 tests[4] reported by Tsai, et al., that FCCI is dominated by lanthanide fission products which have been found at the deepest penetration into cladding [24]. In an alloy system with the presence of lanthanides, the inter-diffusion coefficients and activation energies are both different with those in a system without lanthanides. Fuel smear density and cladding type have significant effects on FCCI. Since the high smear density in the fuel can limit the development of interconnected porosity, which is believed to accelerate the migration of lanthanide fission products, the fuels with lower smear density thereby have higher lanthanide inventory at the fuel/clad interface, leading to more FCCIs [24].

2.2 Out-of-pile analysis

Diffusion couple test is a direct and efficient method to study the diffusion kinetics and chemical reactions of materials. The test is to make solid pieces of pure elements or alloys come into intimate contact and then heat-treat for a period of time, and finally determine the interdiffusion behavior of investigated materials with microstructure characterization analysis. The commonly used microstructure characterization techniques include scanning electron microscope, energy-dispersive spectroscopy, X-ray diffraction, electron probe micro-analysis, wavelength-dispersive spectroscopy, Auger electron spectroscopy, secondary ion mass spectrometry, and Rutherford backscattering spectrometry [1]. The measured composition profiles serve as a good

[4] DP-1 tests contained 61 fuel elements. The fuels included U-19Pu-6Zr, U-19Pu-10Zr, and U-19Pu-14 Zr wt. %, and the cladding types were HT9 and D9. Burnup was about 11 at. %, peak linear power was 53 kW/m, and cladding temperature was 868 K.

source for interdiffusion analysis, as long as the heat-treatment temperature and time duration are known.

Iron is the balance of HT9, its chemical interactions with lanthanide have been broadly studied. On the basis of a diffusion couple test employing mischmetal (70Ce-30La wt. %) and Nd separately coupled with the cladding alloy Fe-9Cr-2W wt. % at 1033 K, it has been found that Ce and Nd diffused into cladding and formed intermetallics, the diffusion kinetics of which followed the parabolic rate law [25,26]. Interactions between lanthanides may increase or decrease the lanthanide-HT9 reaction thickness, depending the specific elements and composition [27,28]. In the quaternary-Ln alloy/HT9 diffusion couple, $Ln_2(Fe,Cr)_{17}$ compounds (Ln here include Nd, Ce, Pr and La) were formed by interdiffusion [21]. The formation of intermetallics at equilibrium condition and the solidus temperature of the system can be found in its *phase diagram*, accordingly, the potential intermetallics formed at the fuel/cladding interface during irradiation are presented in the following. In the Nd-Fe system, Nd_2Fe_{17} and Nd_5Fe_{17} compounds have been reported [29,30], the solidus temperature of Nd-Fe system is at 955 K with 21.7 at. % Fe [31]. In the Ce-Fe system, there are $CeFe_2$ and Ce_2Fe_{17} compounds formed by peritectic reactions, and an eutectic equilibrium presenting in the Ce-rich side [32,33], the solidus temperature of Ce-Fe system is at 865 K with 16.4 at. % Fe. In the Pr-Fe system, only one compound, Pr_2Fe_{17} has been found [34,35], the metastable phase $PrFe_2$ has also been reported but only exists under high pressure [36], the solidus temperature is at 940 K with 18 at. % Fe [35]. In the La-Fe system, there is no intermetallic phase at the atmospheric pressure, the solidus temperature is at 1078 K with 11.4 at. % Fe [37]. In summary, the compounds formed in the Ln-Fe systems have these two compounds: $LnFe_2$ and Ln_2Fe_{17}; except La-Fe system, the solidus temperature of Nd/Ce/Pr-Fe systems is nearly the same as or even lower than the typical fuel/cladding interface temperature (873-923 K), thus susceptible to liquefy.

Chrome is the second major component of HT9. In the Ln-Cr systems, except for some terminal solid phases, there is no compound; the solidus temperature is higher than the typical fuel/cladding interface temperature [38]. The Ln-Cr binary phase may not form during irradiation. Moreover, Cr in HT9 can slow down the Ln-Fe diffusion to some extent. The alloy Fe-20.1Cr and pure Fe metal showed comparable behaviors in the development of a $CeFe_2$ layer at 865 K, the formation of a ternary $Ce_3(Fe,Cr)_7$ phase has been observed due to the presence of Cr in the Fe-20.1Cr/Ce diffusion couple, Cr exhibited the phenomenon of flux reversal at the $Ce_3(Fe,Cr)_7$/Fe interface [39]. The Ce/Fe and Ce/(Fe-Cr-Ni) diffusion couples showed different thicknesses of diffusion layer at 833 K, the thickness decreases with the increasing Cr content, and the Cr-rich phase consisted of Fe and Cr has been found at the front of Ce diffusion path [40]. Therefore, Cr is susceptible to act as a barrier in the interdiffusion between lanthanide and cladding, and slow down the diffusion kinetics.

There is less than 1 wt. % Ni in alloy HT9, however, even a small composition may liquefy as the solidus temperature of Ln-Ni systems is even lower than Ln-Fe systems to some extent. In the Nd-Ni system, many compounds (Nd_3Ni, Nd_7Ni_3, NdNi, $NdNi_2$, $NdNi_3$, Nd_2Ni_7, $NdNi_5$ and Nd_2Ni_{17}) have been found, the solidus temperature of Nd-Ni system is at 857 K with 33.81 at. % Ni, when the range of Ni content is around 19-38 at. %, the solidus temperature is below 973 K [41,42,43]. In the Ce-Ni system, the compounds include Ce_7Ni_2, CeNi, $CeNi_2$, $CeNi_3$, Ce_2Ni_7, and $CeNi_5$, the solidus temperature is at 750-756 K with 21.0 at. % Ni [44,45,46]. In the Pr-Ni system, the compounds include Ni_5Pr, Ni_7Pr_2, Ni_3Pr, Ni_2Pr, NiPr, Ni_3Pr_7 and $NiPr_3$, the solidus temperature is at 822 K with 35.1 at. % Ni [47]. In the La-Ni system, the ompounds include La_3Ni, La_7Ni_3, LaNi, La_2Ni_3, La_7Ni_{16}, $LaNi_3$, La_2Ni_7 and $LaNi_5$, the solidus temperature is around 790 K with 35 at. % [48,49,50].

Figure 2 shows the enthalpy of formation of Ln-Ni and Ln-Fe systems. Enthalpy of formation represents the thermodynamic stability of compounds and the driving force of compound

formation. They are negative, indicating the potential formation of compounds. Ln-Ni compounds and solid phases will be easy to form and grow because the enthalpies of formation are very negative.

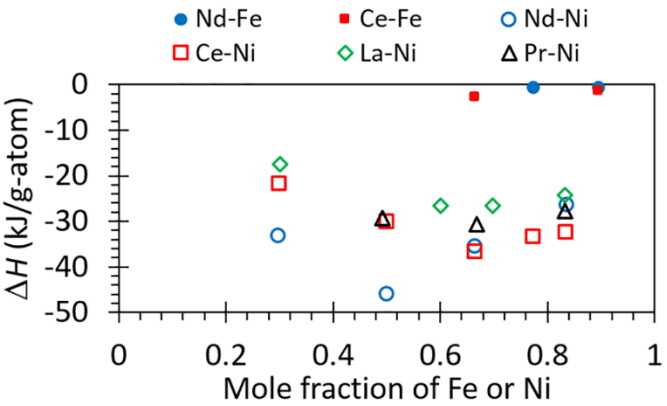

Figure 2 Enthalpy of formation (kJ/g-atom) at 298 K for Ln-Fe and Ln-Ni systems (Ln = Nd, Ce, Pr and La).

3. Lanthanide Migration Theory

As discussed in Section 2, lanthanides at the fuel periphery play important roles in FCCI. During irradiation, lanthanides are generated in fuel, their precipitates at the outer region of fuel and layers of cladding indicate the migration. There are three theories that potentially explain lanthanide migration: solid phase diffusion, vapor phase transport, and liquid-like transport.

Solid phase diffusion theory suggests that lanthanide can migrate in fuel through solid-state diffusion. The differential solubility and diffusion coefficient of lanthanide along the temperature gradient can drive the lanthanide transport. Fundamental data, such as lanthanide solubility and diffusion coefficient are required to estimate the lanthanide migration in the solid fuel matrix. These fundamental data are also dependent on the constituent redistribution during burnup [17]. The diffusion coefficient of Ce in U-Zr solid solution has been measured, which is 2×10^{-13} m^2/s at 1123 K and 6×10^{-14} m^2/s at 1023 K [51]. Since Ce is one of the main compositions of lanthanide fission products, its diffusion behavior is representative. However, these diffusion coefficients are too low, in other words, the solid diffusivity of lanthanide in

fuel matrix is extremely small. This is contrary to the actual lanthanide migration, as suggested by the fast interaction of fuel and cladding at 5 at. % burnup, the actual lanthanide migration is rapid. Accordingly, the solid phase diffusion theory is in doubt to explain the rapid migration process, which must be determined by some other factors.

The vapor transport theory comes up to explain the rapid transport process [52]. The theory is based on the facts that lanthanide can migrate through vapor transport via a network of interconnected porosity even at a very low burnup, the vapor that transports down the temperature gradient to the cladding is attributed to a gradient in fission product vapor pressure from the fuel center to the surface [12]. However, this theory fails in explaining several observations of fuel [18]. An example is that both Ce and Sm have been observed to migrate in spite of a large difference between the vapor pressures of these two elements (approximately eleven orders of magnitude apart) [18]. To more accurately describe the dominant transport mechanism for lanthanide migration, a reverse theory is needed.

The liquid-like transport mechanism [18] has been proposed, indicates that lanthanides are transported through liquid Cs and Na. The theory can explain the lanthanide distribution, precipitation and the rapid migration process. The first contribution to the liquid-like transport is *the liquid Cs and Na filling the interconnected pores and fissures of fuel*. Fuel swelling creates pores and fissures. Cesium as a low melting temperature fission product with low solubility in fuel matrix, accumulates in the pores and fissures. Sodium is a liquid fuel/cladding-gap-filler metal, and fills the porosity of fuel surface. Cesium and sodium together connect the porosity throughout the fuel, being a path to transport lanthanide. In liquid metals, the solubility of lanthanide decreases with decreasing temperature [53], and is lower in liquid Na than in Cs [54], accordingly explains the lanthanide precipitation at the fuel and cladding surfaces.

The other contribution to the liquid-like transport is *the abundance of surface area on the pores and fissures of fuel*. Since lanthanide has low solid-solubility in the fuel matrix, lanthanide

would be expressed from the fuel matrix over time, owing to substantial kinetic energy available from locally high temperature and burnup. Once on the surface of pores, where the lanthanide surface states are weakly bound, lanthanide migration toward the cladding surface will be much more rapid than the solid-solid diffusion would allow. Once the lanthanide contacted cladding, a strong chemical interaction occurs. Thus, once on the fuel periphery, their transport to colder axial zones is also halted. This mode of transport would be enhanced by the presence of liquid Cs, as suggested by the moderate solubility of Dy in Cs. Further, this mode of transport underscores how vapor phase transport is very unlikely; specifically, vapor phase lanthanide would tend to be more uniform (or disposed to colder regions) because of vapor mobility and immediate strong chemical interaction that pin the lanthanide on the cladding.

The liquid-like transport theory has been validated through experimental measurements [8] and modeling simulations [55]. Investigations were focused on lanthanide solubility and diffusivity in liquid Cs, Na and Na-Cs mixtures. Solubilities of Nd, Ce and La in the liquids have been measured at different temperatures [8]. One example of solubility of Nd in the liquids is shown in Figure 3. It indicates that the Nd solubility in liquid Cs is much higher than in Na. At 723 K, the solubility in Cs is more than two orders larger than in Na, the temperature drop also makes solubility decreases in orders (Figure 3a). In the liquid Na-Cs mixtures, the solubility decreases with the increase of Na concentration (Figure 3b). Under irradiation, the concentration of Cs in the interconnected pores and fissures is higher in the fuel interior region than the outer region because Cs is produced as a fission product and its amount is affected by burnup; meanwhile, the concentration of Na in the outer region is higher than Cs, considering Na is the gap filler. Accordingly, lanthanides produced during irradiation primarily dissolve in the liquid Cs, and then transport outside driven by the concentration gradient; with the increase of Na in the outer region, lanthanides become difficult to dissolve and thus precipitate. As observed on the fuel surface, lanthanide precipitates have an appearance of “sludge-like”, indicating swift

solidification with no exhibition of crystal characteristics [18], this is in contrast to the other fission product precipitates with uniformly shaped cubic structures [56]. These behaviors indicate that lanthanide precipitation is a rapid process, the sudden drop of solubility caused by the increase of Na concentration and the decrease of temperature cannot afford enough time for lanthanide to form a crystal structure.

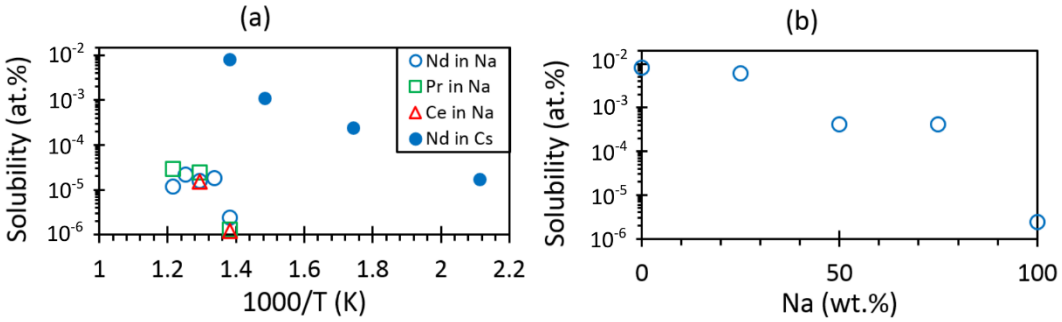

Figure 3 (a) solubility of Nd, Pr and Ce in liquid Na and liquid Cs at different temperatures, (b) solubility of Nd in liquid Cs-Na mixtures at 723 K [8].

The lanthanides that migrate to the fuel surface have two ways to transport to the cladding surface, one is *fuel swelling that makes lanthanide-cladding directly contacted*, the other is *lanthanide diffusion through the Na-filled gap*. A simulation model based on *ab-initio* molecular dynamics has been developed to calculate the diffusion coefficients of Nd, Ce and Pr in liquid Na and Cs [55,57]. Results are summarized in Figure 4. Diffusion coefficients are in the order of 10^{-5} cm^2/s. The diffusion coefficient of a give lanthanide is always higher in liquid Na than Cs. The higher diffusion coefficient in liquid Na makes it possible for lanthanides to pass through the Na-filled gap. The diffusion coefficient decreases with decreasing temperature, so the lanthanide will finally deposit on the cladding surface. The simulation using BISION code has shown the transport of lanthanide from the fuel center to the edge through Cs-filled cracks, and the deposition of lanthanide on fuel and cladding surfaces [55].

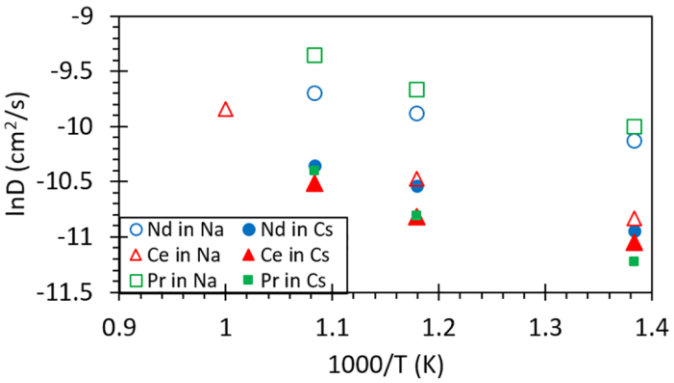

Figure 4 Diffusion coefficients of Nd, Ce and Pr in liquid Na and Cs [55].

In summary, lanthanides primarily dissolve in the liquid Cs-filled pores and fissures of fuel, transport from the inner region to the outer driven by concentration and temperature gradients, some of them rapidly precipitate in the fuel outer region (note the "sludge-like" lanthanide precipitates) because of the sudden drop of solubility caused by the increase of liquid Na concentration. The lanthanides on the fuel surface will either directly contact with cladding by fuel swelling, or deposit on cladding through diffusion in the Na-filled gap.

4. Immobilizing lanthanides with fuel additives

Some concepts which aim to create a physical barrier between the fuel (including lanthanide fission products) and cladding have been evaluated over the past several decades, including using different types of fuel and clad, creating diffusion barriers (e.g. Zr-rich "rind") and cladding liners; however, none of them was able to solve the FCCI problem adequately [6]. The more active concept, which focuses on minimizing lanthanide migration in the irradiated fuel, is to add a small amount of additive dopants into the fuel alloy to bind lanthanides into intermetallic compounds [18][58][59]. The dopant candidates must have these properties: low fast neutron cross section, high affinity with lanthanide to form stable compound, weak chemical reaction with fuel constituents, low additive-to-lanthanide stoichiometry, and uniform

distribution in the fuel [18,59]. Accordingly, the candidate fuel additives include Sb [60], Pd [18], Sn [61], Te [62] and In [59].

In U-Zr-Sb alloys, uniformly distributed precipitates that consist of Zr_2Sb compound and Zr-rich Zr-U-Sb phase have been observed [60]. The U-Zr-Sb-Ce alloys have also been analyzed, they were cast by adding the appropriate amount of Ce in the pre-alloy of U-Zr-Sb. In U-Zr-Sb-Ce alloys, Ce_4Sb_3 and Ce_2Sb compounds have been observed, while the pre-formed Zr-Sb phases in the pre-alloy of U-Zr-Sb were not found. The results indicate that Sb can release Zr from the Zr-Sb phases back to the fuel matrix, and Sb can combine with Ce to form stable compounds Ce_4Sb_3 and Ce_2Sb. Antimony appears to have a preference for Ce over Zr because the enthalpies of formation of Sb-Ce compounds are greatly negative, the driving force of formation is high. In U-Zr-Pd-Ln alloys (here Ln = 53Nd–25Ce–16Pr–6La wt. %), Palladium collocated with Ln in the ratio of 1:1 at most regions [18]. Diffusion couple tests that jointed Fe disc with 50Pd-50Ln disc (here Ln is Nd, Ce or Pr) have found that Pd significantly increased the stability of these lanthanides toward Fe [58]. Similarly, in U-Zr-Sn-Ln alloys, Sn collocated with Ln in the forms of Ln_5Sn_3 and possibly $(Ln,Zr)_5Sn_3$ [61]. Indium displayed similar behaviors to Pd and Sn [59]. However, Pd, Sn and In did not fully release Zr back to the fuel matrix like Sb did, instead, they consumed a fraction of Zr and formed Pd/Sn/In-Zr-Ln precipitations in the alloys. It has not been determined whether these intermetallics are Zr-included, or Zr is one element of the ternary compound. Either way, the Zr content is lessened in the fuel matrix, lowering the fuel solidus temperature. Among these candidate additive dopants, Sb appears to show high binding preference for lanthanides while effectively releasing Zr back to the fuel matrix.

Except for the advantages of immobilizing lanthanides in the fuel, the fuel additive is also expected to play a role in raising the solidus temperature when lanthanides contact with cladding. The solidus temperature of the binary Ln-X system (Ln = Nd, Ce, Pr or La, X = Fe or Ni) is

susceptible to be elevated with the additive. Despite the phase equilibria in the Ln-X-additive ternary systems has not been sufficiently established, the known ternary systems have indicated an academic basis for implementing the forecast. Most of Ln-X-additive ternary systems show stable intermetallics without liquid phase at the typical fuel/cladding interface temperature.

In the Nd-Fe-Sb system, five ternary compounds $Nd_6Fe_{13}Sb$, $NdFe_{0.6}Sb_2$, $Nd_2Fe_{3.52}Sb_{4.88}$ (or $Nd_2Fe_{3.96}Sb_{4.97}$), $Nd_3Fe_3Sb_7$ and $NdFeSb_3$ as well as the liquid phase have been found at 1073 K [63]. All the crystal structure data have been established, but thermodynamic data are lacking.

In the Ce-Fe-Sb system, three ternary compounds $CeFe_4Sb_{12}$, $CeFeSb_2$ and $Ce_2Fe_4Sb_5$ have been found at 1173 K [64] and 823 K [65], however, the established isothermal section showing the compound $FeSb_2$ at 1173 K is in doubt, as $FeSb_2$ should not exist at this temperature. Recent simulation using CALPHAD method has confirmed the ternary compounds at 973 K, and liquid phase is not present [66]. In the La-Fe-Sb system, two ternary compounds $LaFe_4Sb_{12}$ and $LaFe_2Sb_2$, twelve single-phase regions, twenty-three two-phase regions and twelve three-phase regions have been found at 773 K, liquid phase was not found at the temperature [67]. Crystal data of all the compounds have been established, but thermodynamic data are lacking.

In the Ln-Ni-Sb systems (here Ln = Nd, Ce, Pr and La), the compounds $LnNiSb_2$ with their crystal structure have been found at 873 K [68], $LnNi_{2-x}Sb_2$ with their crystal structure have been found at 1023-1073 K [69]. LnNiSb with their crystal structure have been found at 973 K [70] and 1123 K [71]. Except for these compounds, some other compounds in the systems have also been reported. In the Ce-Ni-Sb system, $CeNiSb_3$ has been found by heating at 1123 K for 7 days followed by annealing at 873 K for 5 days [72]. In the Pr-Ni-Sb system, five ternary compounds $PrNiSb_3$, $PrNi_{0.62-1.35}Sb_2$, $PrNi_2Sb_2$, PrNiSb, Pr_5NiSb_2 and a homogeneity region $PrNi_{2+x}Sb_{2-y}$ have been found at 870 K; liquid phase was not found at the temperature [73].

Compared with Ln-Fe and Ln-Ni binary systems as discussed in Section 2.2, the Ln-Fe/Ni-Sb ternary systems appear to have higher solidus temperatures, for examples, Ce-Fe system melts

at 865 K, while Ce-Fe-Sb system does not melt even at 973 K; Pr-Ni system melts at 822 K, while Pr-Ni-Sb system does not melt even at 870 K. However, thermodynamic data of these systems are insufficient to support the conclusion, more investigations on the solidus temperature of ternary systems as well as the driving force of compound formation are needed.

5. Conclusion

The present review focuses on the roles of lanthanide fission products on FCCIs. Based on the analysis and review of available experimental data (both in-pile and out-of-pile data), the formation of low-melting alloys between lanthanides and Fe and Ni is the major mechanism that leads to lanthanide-involved FCCIs. For lanthanide migration in the fuel, the liquid-like transport theory that explains the lanthanide distribution, precipitation and rapid migration process is the most credible. For reducing FCCIs, immobilizing lanthanide by adding fuel additives is an effective way. Among all the candidate additives, Sb appears to have the most advanced characteristics based on available experimental data.

Although the mechanisms of lanthanide-involved FCCIs are well understood, more research is still needed for mitigating FCCIs and improving the fuel performance. Current available studies indicate that using fuel additives is an effective method for mitigating FCCIs. However, all those data were from out-of-pile diffusion-couple tests or microstructure characterization of non-irradiated alloys. Therefore, irradiation tests of U-Zr fuel with additives should be performed. How to fabricate the fuel with additives is another research topic that needs more investigation. Some additives (e.g. Te) have low melting and boiling temperatures, so casting may lead loss of additives. Effects of additives on the fresh fuel properties such as mechanical properties as well as effects of additive-Zr precipitates formed during fuel fabrication should be fully understood before using additives for mitigating FCCIs. Research may focus on the amount of Zr consumed by an additive, the Zr concentration in fuel matrix and the corresponding melting temperature. Heat-treatment that may cause precipitates transformation

and porosity and void formation also need to be studied. The thermodynamic stability of additive-lanthanide compounds, formed through the alloy fabrication, were studied based on microstructure characterization of U-Zr alloy with additives and lanthanides. While in a nuclear reactor, the kinetics of compound formation are important as the lanthanide fission products are continuously produced. However, such kinetics data are very scarce and need to be studied.

Acknowledgement

The authors acknowledge the financial support of U.S. Department of Energy Nuclear Energy University Program [grant number DE-NE0008574 and DE-NE0008283].

References

1 F. Delage, J. Carmack, C.B. Lee, T. Mizuno, M. Pelletier, J. Somers, *J. Nucl. Mater.* **2013**, *441*, 515.

2 W.J., Carmack, D.L. Porter, Y.I. Chang, S.L. Hayes, M.K. Meyer, D.E. Burkes, C.B. Lee, T. Mizuno, F. Delage, J. Somers, *J. Nucl. Mater.* **2009**, *392*, 139.

3 W.J. Carmack, H.M. Chichester, D.L. Porter, D.W. Wootan, *J. Nucl. Mater.* **2016**, *473*, 167.

4 R.G. Pahl, D.L. Porter, D.C. Crawford, L.C. Walters, *J. Nucl. Mater.* **1992**, *188*, 3.

5 G.L. Hofman, L.C. Walters, T.H. Bauer, *Prog. Nucl. Energy* **1997**, *31*, 83.

6 D.D. Keiser, Technical Report ANL-NT-240, Argonne National Laboratory - West, Idaho Falls, ID, **2006**.

7 G.L. Hofman, S.L. Hayes, M.C. Petri, *J. Nucl. Mater.* **1996**, *227*, 277.

8 J. Isler, Interactions of Lanthanides and Liquid Alkali Metals for liquid-like Lanthanide Transport in U-Zr Fuel. Master Thesis, The Ohio State University, **2017**.

9 G.L. Hofman, R.G. Pahl, C.E. Lahm, D.L. Porter, *Metall. Trans. A* **1990**, *21*, 517.

10 Y.S. Kim, G.L. Hofman, A.M. Yacout, *J. Nucl. Mater.* **2009**, *392*, 164.

11 R.D. Mariani, D.L. Porter, S.L. Hayes, J.R. Kennedy, *Procedia Chem.* **2012**, *7*, 513.

12 R.G. Pahl, C.E. Lahm, S.L. Hayes, *J. Nucl. Mater.* **1993**, *204*, 141.

13 D.D. Keiser, M.C. Petri, *J. Nucl. Mater.***1996**, *240*, 51.

14 C. Matthews, C. Unal, J. Galloway, D.D. Keiser, S.L. Hayes, *Nucl. Technol.* **2017**, *198*, 231.

15 D.H. Tsai, Fuel/cladding compatibility in irradiated metallic fuel pins at elevated temperatures, in: International topical meeting on fast reactor safety, Snowbird, UT, **1990**.

16 A.B. Cohen, H. Tsai, L.A. Neimark, *J. Nucl. Mater.* **1993**, *204*, 244.

17 C.W. Arnold, J. Galloway, C. Unal, Modeling lanthanide transport in metallic fuels with BISON, Global 2015, International Fuel Cycle Conference proceedings, Paper 5084, Paris, France, September 21-24, **2015**.

18 R.D. Mariani, D.L. Porter, T.P. O'Holleran, S.L. Hayes, J.R. Kennedy, *J. Nucl. Mater.* **2011**, *419*, 263.

19 A. Itoh, M. Akabori, K. Nakamura, T. Ogata and T. Ogawa, Proc. 1997 Fall Meeting of the Atomic Energy Society of Japan, **1997**, *I66*, 708 [in Japanese].

20 R.G. Pahl, D.L. Porter, C.E. Lahm, G.L. *Hofman, Metall. Trans. A* **1990**, *21*, 1863.

21 J.H. Kim, J.S. Cheon, J.H. Kim, B.O. Lee, C.B. Lee, *Met. Mater. Int.* **2014**, *20*, 819.

22 T. Ogata, M. Kurata, K. Nakamura, A. Itoh, M. Akabori, *J. Nucl. Mater.* **1997**, *250*, 171.

23 G. Bozzolo, H.O. Mosca, A.M. Yacout, G.L. Hofman, *J. Nucl. Mater.* **2010**, *407*, 228.

24 H. Tsai, A.B. Cohen, M.C. Billone, L.A. Niemark, Irradiation Performance of U-Pu-Zr Metallic fuels for Liquid Metal-Cooled Reactors, in: 3rd International Conference on Nuclear Engineering (ICONE-3), Kyoto, Japan, April 23-27, **1995**.

25 J.H. Kim, B.O. Lee, C.B. Lee, S.H. Jee, Y.S. Yoon, *J. Rare Earths* **2012**, *30*, 599.

26 J.H. Kim, J.H. Baek, B.O. Lee, C.B. Lee, Y.S. Yoon, *Met. Mater. Int.* **2011**, *17*, 535.

27 J.H. Kim, J.S. Cheon, B.O. Lee, J.H. Kim, *J. Nucl. Mater.* **2016**, *479*, 394.

28 E.B. Lee, B.O. Lee, W. Shim, J.H. Kim, *Nucl. Eng. Technol.* **2018**, *50*, 915.

29 J.M. Moreau, L. Paccard, *J. Less-Common Met*. **1990**, *163*, 245.

30 K. Pawlik, J.J. Wyslocki, J. Olszewski, O.I. Bodak, P. Pawlik, *Proc. of Nukleonika* **2004**, *49*, S27.

31 M.-A.V. Ende, I.-H. Jung, *J. Alloys Compd.* **2013**, *548*, 133.

32 Y.C. Chuang, C.H. Wu, Z.B. Shao, *J. Less-Common Met.* **1987**, *136*, 147.

33 X. Su, J.-C. Tedenac, *Calphad* **2006**, *30*, 455.

34 Q. Johnson, D.H. Wood, G.S. Smith, *Acta Crystallogr.* **1968**, *B24*, 274.

35 W. Zhang, C. Li, X. Su, *J. Phase Equilib.* **1999**, *20*, 158.

36 J.F. Cannon, D.L. Robertson, H.T. Hall, *Mater. Res. Bull.* **1972**, *7*, 5.

37 E. Provoden-Karadeniz, A.N. Grundy, M. Chen, T. Ivas, L.J. Gauckler, *J. Phase Equilib. Diffus.* **2009**, *30*, 351.

38 S. Ray, J.P. Neumann, *J. Phase Equilib.* **1996**, *17*, 179.

39 P.C. Tortorici, M.A. Dayananda, *J. Nucl. Mater.* **1993**, *204*, 165.

40 W. Lo, N. Silva, Y. Wu, R. Winmann-Smith, Y. Yang, *J. Nucl. Mater.* **2015**, *458*, 264.

41 Y. Du, N. Clavaguera, *Calphad* **1996**, *20*, 289.

42 M. Huang, R.W. McCallum, T.A. Lograsso, *J. Alloys Compd.* **2005**, *398*, 127.

43 Q. Luo, S.-L. Chen, J.-Y. Zhang, L. Li, K.-C. Chou, Q. Li, *Calphad* **2015**, *51*, 282.

44 Z. Du, L. Yang, G. Ling, *J. Alloys Compd.* **2004**, *375*, 186.

45 M. Palumbo, G. Borzone, S. Delsante, N. Parodi, G. Cacciamani, R. Ferro, L. Battezzati, M. Baricco, *Intermetallics* **2004**, *12*, 1367.

46 W. Xiong, Y. Du, X. Lu, J.C. Schuster, H. Chen, *Intermetallics* **2007**, *15*, 1401.

47 Z. Rahou, K. Mahdouk, D. Moustain, S. Otmani, S. Kardellass, A. Iddaoudi, N. Selhaoui, *J. Alloys Compd.* **2015**, *620*, 204.

48 Z. Du, D. Wang, W. Zhang, *J. Alloys Compd.* **1998**, *264*, 209.

49 J. Dischinger, H.-J. Schaller, *J. Alloys Compd.* **2000**, *312*, 201.

50 H. Okamoto, *J. Phase Equilib.* **1991**, *12*, 615.

51 T. Ogata, M. Akabori, A. Itoh, *Mater. Trans.* **2003**, *44*, 47.

52 G.L. Hofman, L.C. Walters, Metallic fast reactor fuels, in Materials Science and Technology: A Comprehensive Treatment, R.W. Cahn, P. Haasen, E.J. Kramer (Eds.), *10A*, **1994**.

53 H.E. Johnson, et al., Na-NaK Engineering Handbook, vol. 1, O.J. Foust (Ed.), New York, N.Y.: Gordon and Breach Science Publishers Inc, **1972**.

54 G.J. Lamprecht, P. Crowther, *Trans. of the Met. Society of AIME*. **1968**, *242*, 2169.

55 X. Li, Studies of Liquid-like Lanthanide Transport Behaviors in Metallic Nuclear Fuels, Ph.D Dissertation, The Ohio State University, **2017**.

56 D.D. Keiser Jr., R.D. Mariani, *J. Nucl. Mater.* **1999**, *270*, 279.

57 X. Li, A. Samin, J. Zhang, C. Unal, R.D. Mariani, *J. Nucl. Mater.* **2017**, *484*, 98.

58 G.W. Egeland, R.D. Mariani, T. Hartmann, D.L. Porter, S.L. Hayes, J.R. Kennedy, *J. Nucl. Mater.* **2013**, *440*, 178.

59 Y.S. Kim, T. Wiencek, E. O'Hare, J. Fortner, A. Wright, J.S. Cheon, B.O. Lee, *J. Nucl. Mater.* **2017**, *484*, 297.

60 Y. Xie, M.T. Benson, J.A. King, R.D. Mariani, J. Zhang, *J. Nucl. Mater.* **2018**, *498*, 332.

61 M.T. Benson, J.A. King, R.D. Mariani, M.C. Marshall, *J. Nucl. Mater.* **2017**, *494*, 334.

62 Y. Xie, J. Zhang, M.T. Benson, J.A. King, R.D. Mariani, Assessment of Te as a U-Zr fuel additive to mitigate fuel-cladding chemical interactions. *J. Nucl. Mater.* (under review), **2019**.

63 N. Nasir, A. Grytsiv, P. Rogl, D. Kaczorowski, H.S. Effenberger, *Intermetallics* **2010**, *18*, 2361.

64 J.W. Kaiser, W. Jeitschko, *J. Alloys Compd.* **1999**, *291*, 66.

65 D. Zhu, C. Xu, C. Li, C. Guo, R. Zheng, Z. Du, J. Li, *J. Alloys Compd.* **2018**, *731*, 1125.

66 Y. Xie, J. Zhang, Thermodynamic modeling of lanthanide-cladding-additive systems: Assessment of the Ce-Fe-Sb system, Transactions of the American Nuclear Society, 2017 ANS Winter Conference, Washington, DC, Oct. 29-Nov.2, **2017**.

67 J. Liu, L.Wang, X. Cui, W. Liu, B. Zong, J. Li, *J. Alloys Compd.* **2008**, *456*, 135.

68 O. Sologub, K. Hiebl, P. Rogl, H. Noel, O. Bodak, *J. Alloys Compd*. **1994**, *210*, 153.

69 W.K. Hofmann, W. Jeitschko, *J. Less-Common Met.* **1988**, *138*, 313.

70 I. Karla, J. Pierre, R.V. Skolozdra, *J. Alloys Compd.* **1998**, *265*, 42.

71 K. Hartjes, W. Jeitschko, *J. Alloys Compd.* **1995**, *226*, 81.

72 R.T. Macaluso, D.M. Wells, R.E. Sykora, T.E. Albrecht-Schmitt, A. Mar, S. Nakatsuji, H. Lee, Z. Fisk, J. Y. Chan, *J. Solid State Chem.* **2004**, *177*, 293.

73 S.I. Chykhrij, V.B. Smetana, *J. Alloys Compd.* **2005**, *400*, 100.